

## Raman fingerprint of charged impurities in graphene

C. Casiraghi<sup>a)</sup> and S. Pisana

Engineering Department, Cambridge University, Cambridge CB3 0FA United Kingdom

K. S. Novoselov and A. K. Geim

Department of Physics and Astronomy, Manchester University, Manchester M13 9PL, United Kingdom

A. C. Ferrari<sup>b)</sup>

Engineering Department, Cambridge University, Cambridge CB3 0FA, United Kingdom

(Received 19 September 2007; accepted 7 November 2007; published online 5 December 2007)

We report strong variations in the Raman spectra for different single-layer graphene samples obtained by micromechanical cleavage. This reveals the presence of excess charges, even in the absence of intentional doping. Doping concentrations up to  $\sim 10^{13} \text{ cm}^{-2}$  are estimated from the  $G$  peak shift and width and the variation of both position and relative intensity of the second order  $2D$  peak. Asymmetric  $G$  peaks indicate charge inhomogeneity on a scale of less than  $1 \mu\text{m}$ . © 2007 American Institute of Physics. [DOI: 10.1063/1.2818692]

Graphene is the prototype two-dimensional carbon system<sup>1</sup> and a promising candidate for future electronics.<sup>2–4</sup> Graphene samples are usually obtained from micromechanical cleavage of graphite<sup>5</sup> and they can be identified by elastic and inelastic light scattering, such as Rayleigh and Raman spectroscopies.<sup>6,7</sup>

Raman spectroscopy is a fast and nondestructive method for the characterization of carbons.<sup>8</sup> Their Raman spectra show common features in the  $800\text{--}2000 \text{ cm}^{-1}$  region: the  $G$  and  $D$  peaks, which lie at around  $1560$  and  $1360 \text{ cm}^{-1}$ , respectively. The  $G$  peak corresponds to the  $E_{2g}$  phonon at the Brillouin zone center. The  $D$  peak is due to the breathing modes of  $sp^2$  atoms and requires a defect for its activation.<sup>9–11</sup> It is common for as-prepared graphene not to have enough structural defects for the  $D$  peak to be Raman active,<sup>7</sup> so that it can only be seen at the edges.<sup>7</sup> However, the most prominent feature in graphene is the second order of the  $D$  peak: the  $2D$  peak.<sup>7</sup> This lies at  $\sim 2700 \text{ cm}^{-1}$  and it is always seen, even when no  $D$  peak is present, since no defects are required for the activation of second order phonons. Its shape distinguishes single and multilayer samples. Graphene has a sharp, single  $2D$  peak, in contrast with graphite and few-layers graphene.<sup>7</sup>

The ability to controllably dope  $n$  or  $p$  is key for applications. Raman spectroscopy can monitor doping in graphene.<sup>12,13</sup> The effect of back gating and top gating on the  $G$ -peak position [ $\text{Pos}(G)$ ] and its full width at half maximum [ $\text{FWHM}(G)$ ] was reported in Refs. 12–14.  $\text{Pos}(G)$  increases and  $\text{FWHM}(G)$  decreases for both electron and hole dopings. The stiffening of the  $G$  peak is due to the nonadiabatic removal of the Kohn anomaly at  $\Gamma$ .<sup>12,15</sup> The  $\text{FWHM}$  sharpening is due to blockage of the phonon decay into electron-hole pairs due to the Pauli exclusion principle, when the electron-hole gap becomes higher than the phonon energy.<sup>12,16</sup>  $\text{FWHM}(G)$  sharpening saturates when doping causes a Fermi level shift bigger than half the phonon energy.<sup>12,14</sup> A similar behavior is observed for the  $\text{LO-}G^-$  peak in metallic nanotubes<sup>17,18</sup> for the same reasons.

Most of the previous research focused on the properties of well defined graphene layers and devices<sup>1,4–7,12–14,19,20</sup> with little effort on a systematic investigation of sample variability. Here, we show that Raman spectroscopy can fingerprint differences between nominally identical samples produced in the same way. We find that, even in the absence of a  $D$  peak, changes in the Raman parameters are most common and relate to the presence of excess charges. This is a significant finding, which reconciles the variation of electrical properties often found for nominally identical samples.

We study more than 40 as-prepared monolayer graphenes, produced by microcleavage of graphite. These have different areas, from few  $\mu\text{m}^2$  to  $450 \mu\text{m}^2$ . Some of them are also measured in a device configuration after deposition of Au electrodes (with a thin Cr underlayer). More than  $\sim 100$  spectra are measured using a  $100\times$  objective at  $514$  and  $633 \text{ nm}$ , with a Renishaw spectrometer, of  $\sim 2 \text{ cm}^{-1}$  spectral resolution and power well below  $2 \text{ mW}$ .

Figure 1(a) plots the  $514 \text{ nm}$  spectra of different samples normalized to the  $G$  peak. The  $G$  peak significantly shifts. The  $2D$  peak also shows a small change in position. The relative intensity of the  $2D$  and  $G$  peaks strongly varies. Figure 1(b) plots spectra measured on the same graphene sample. This is a contacted sample, and the spectra change moving closer to the electrodes. Figure 1(c) indicates that the  $G$  peak can be sometimes asymmetric. Note that Fig. 1 does not mean that the Raman spectra always vary in different samples or that they always change within a given sample. However, it warns that uniformity has to be checked, and cannot be simply assumed. Moreover, Fig. 1 dismisses the suggestion of Refs. 21 and 22 that either  $G$  peak position or  $I(2D)/I(G)$  can be used to estimate the number of layers, since the variation of these parameters in as deposited single layers far exceeds that assigned to the increase of number of layers.<sup>21,22</sup> Note that the criterium based on the shape of the  $2D$  peak<sup>7</sup> still stands and allows layer counting.

Figure 2 plots  $\text{Pos}(G)$  and  $\text{FWHM}(G)$ . There is a clear correlation: a  $\text{Pos}(G)$  increase corresponds to a  $\text{FWHM}(G)$  decrease. This is quite similar to what we observed in intentionally doped graphene, where the Fermi energy was modulated using a gate.<sup>12,13</sup> Indeed, the continuous line in Fig. 2 plots the theoretical correlation between  $\text{Pos}(G)$  and  $\text{FWHM}(G)$  obtained from combining Eqs. (6) and (7) of

<sup>a)</sup>Current Address: Physics dep., Freie Universität, Arnimallee 14, D-14195 Berlin, Germany.

<sup>b)</sup>Electronic mail: acf26@eng.cam.ac.uk.

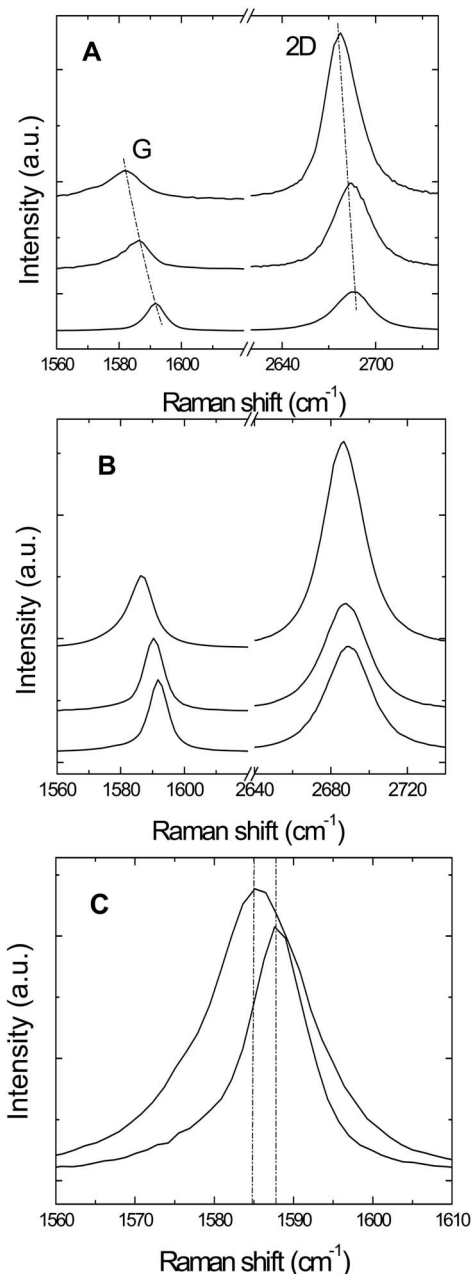


FIG. 1. (a) 514 nm spectra of three different graphene samples. (b) Spectra in three different points of the same sample. (c) The G peak can sometimes be asymmetric.

Ref. 12. The agreement with experiments is remarkable considering that Ref. 12 studied a single sample as a function of doping, while Fig. 2 is a collection of measurements on tens of different samples with no intentional control of doping. The star data points in Fig. 2 are measurements on contacted samples. Interestingly, they usually have significant doping. This is consistent with chemical doping during microfabrication procedures, which can often be seen as a shift of the charge neutrality point away from zero gate voltage.<sup>12–14,19,23,24</sup> However, it is quite remarkable that “pristine” samples, with no contacts, exhibit almost an order of magnitude doping variation, with a few showing a very high doping over  $\sim 10^{13}$  cm<sup>-2</sup>. Excess charges can be due to substrate, adsorbates, and resist/process residuals.<sup>29</sup> In contacted samples, the difference of work function between sample and contacts can also contribute to the doping variation across the layer.

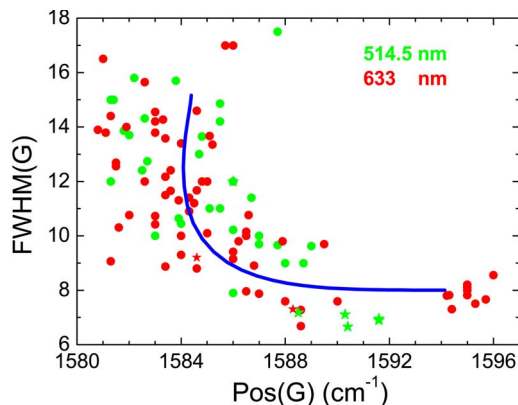


FIG. 2. (Color online) FWHM(G) and Pos(G) at 514 and 633 nm. Stars indicate samples with metallic contacts. Only spectra without D peak are fitted. The solid line is the theory for doped graphene at 300 K (Ref. 12), giving more than  $10^{13}$  cm<sup>-2</sup> doping for the bottom-right samples (Refs. 12 and 13).

Figure 2 shows that the maximum FWHM(G) for the most intrinsic samples is  $\sim 16$  cm<sup>-1</sup>, slightly higher than in graphite.<sup>16,25</sup> Note that all spectra used to derive Fig. 2 do not show any D peak. Thus, we exclude a significant influence of defects in the measured trend. Interestingly, as already observed in Refs. 12 and 14, FWHM(G) never becomes smaller than  $\sim 6$  cm<sup>-1</sup>, while for very high doping we would expect the minimum FWHM(G) to be close to our spectral resolution ( $\sim 2$  cm<sup>-1</sup>). This implies an inhomogeneous distribution of charges within the laser spot of  $\sim 1$   $\mu\text{m}^2$  even for high self-doping, or a non-adiabatic increase of anharmonicity for high doping. The asymmetric spectra of Fig. 1(c) indicate even larger variations.

Figure 3 includes data from samples with a D peak. Some fall in the same FWHM(G)/Pos(G) relation for D-peak-free samples, indicating that they originate from sample edges, not from disorder. However, others have FWHM(G) above 16 cm<sup>-1</sup>, the maximum measured for D-peak-free samples, accompanied by a stiffening of the G peak. This is a signature of structural disorder.<sup>10,26,27</sup> Indeed, in the case of graphite, it is known that, for increasing defects leading to nanocrystalline graphite, FWHM(G) and Pos(G) both increase,<sup>10,26,27</sup> the opposite of what happens for increasing doping. Thus, a large FWHM(G), together with Pos(G) close to 1580 cm<sup>-1</sup> and no D peak, fingerprint the most intrinsic samples, while a large FWHM(G), Pos(G)

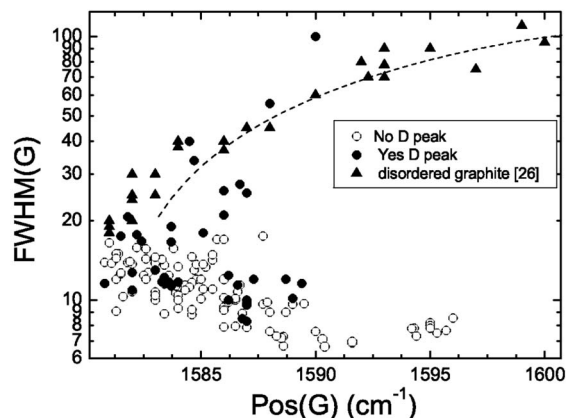


FIG. 3. FWHM(G) and Pos(G) for graphene with and without D peak and for nanocrystalline graphite (Ref. 26).

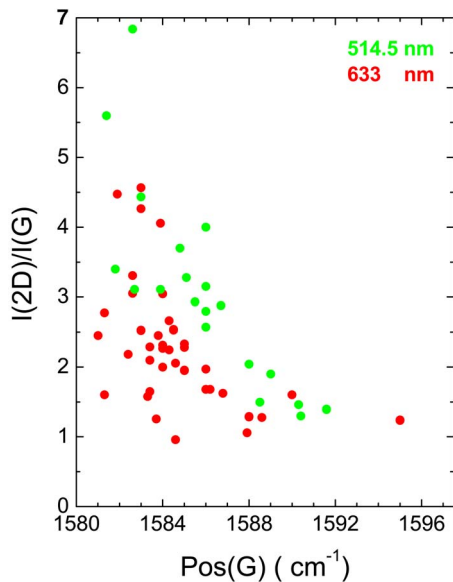


FIG. 4. (Color online)  $I(2D)/I(G)$  as a function of  $\text{Pos}(G)$ .

higher than  $1580\text{ cm}^{-1}$  and a  $D$  peak indicate structural disorder.

We now analyze the  $2D$  peak. Figure 4 plots  $I(2D)/I(G)$  as a function of  $\text{Pos}(G)$ . This clearly shows a large variation with doping: at low doping the  $2D$  peak is 3–5 times stronger than the  $G$  peak, depending on the excitation wavelength; at high doping (for a  $G$  peak position above  $1592\text{ cm}^{-1}$ ) the intensity ratio is  $\sim 1$ .

Figure 5 correlates  $\text{Pos}(2D)$  and  $\text{Pos}(G)$ . Unlike the  $G$  peak, the  $2D$  peak always upshifts with excitation energy due to double resonance.<sup>7,11</sup> The dispersion with excitation energy is  $95\text{--}85\text{ cm}^{-1}/\text{eV}$ . Figure 5 also shows that the  $2D$  peak is sensitive to doping. Doping has two major effects: (i) modification of the equilibrium lattice parameter with a consequent stiffening/softening of the phonons,<sup>28</sup> and (ii) onset of dynamic effects beyond the Born-Oppenheimer approximation that modify the phonon dispersions close to the Kohn anomalies.<sup>12,15</sup> For the  $2D$  peak, the influence of dynamic effects is expected to be negligible, since the  $2D$  phonons are far away from the Kohn anomaly at  $K$ .<sup>7,13,25</sup> Thus, the variation of the  $2D$  peak with doping is mainly due to charge transfer, with hole doping resulting in an upshift, and the opposite for high electron doping.<sup>13</sup> Indeed,  $\text{FWHM}(2D)$  does not show the same trend as  $\text{FWHM}(G)$ , but is

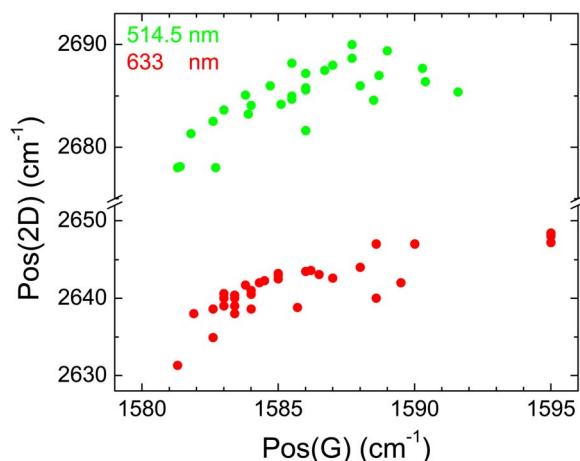


FIG. 5. (Color online)  $\text{Pos}(2D)$  as a function  $\text{Pos}(G)$  at 514 and 633 nm.

$\sim 28\text{--}30\text{ cm}^{-1}$  for all samples. Since Fig. 5 indicates  $2D$  stiffening with increasing  $\text{Pos}(G)$ , we conclude that most of our samples show hole doping. This agrees with what found in electrical measurements, where the charge neutrality points are mostly reached for positive gate bias.<sup>13,19</sup> Adsorbants induce chemical doping and water could explain the  $p$  doping.<sup>29</sup>

In conclusion, we presented a systematic analysis of the Raman spectra of as-deposited graphene. When no  $D$  peak is present, the large variation in Raman parameters is assigned to charged impurities. Variations in the Raman spectra can also be observed within the same sample, indicating inhomogeneous charges. A  $D$  peak far from the edge means structural disorder. Thus, Raman is a powerful tool to monitor the “quality” of graphene.

C.C. acknowledges the Oppenheimer Fund. ACF, AKG, KSN the Royal Society, and Leverhulme Trust.

- <sup>1</sup>A. K. Geim and K. S. Novoselov, *Nat. Mater.* **6**, 183 (2007).
- <sup>2</sup>M. Y. Han, B. Ozyilmaz, Y. Zhang, and P. Kim, *Phys. Rev. Lett.* **98**, 206805 (2007).
- <sup>3</sup>M. C. Lemme, T. J. Echtermeyer, M. Baus, and H. Kurz, *IEEE Electron Device Lett.* **28**, 282 (2007).
- <sup>4</sup>Z. Chen, Y. M. Lin, M. J. Rooks, and P. Avouris, e-print arXiv:cond-mat/0701599.
- <sup>5</sup>K. S. Novoselov, D. Jiang, F. Schedin, T. J. Booth, V. V. Khotkevich, and S. V. Morozov, *Proc. Natl. Acad. Sci. U.S.A.* **102**, 10451 (2005).
- <sup>6</sup>C. Casiraghi, A. Hartschuh, E. Lidorikis, H. Qian, H. Harutyunyan, T. Gokus, K. S. Novoselov, and A. C. Ferrari, *Nano Lett.* **7**, 2177 (2007).
- <sup>7</sup>A. C. Ferrari, J. C. Meyer, V. Scardaci, C. Casiraghi, M. Lazzeri, F. Mauri, S. Piscanec, D. Jiang, K. S. Novoselov, S. Roth, and A. K. Geim, *Phys. Rev. Lett.* **97**, 187401 (2006).
- <sup>8</sup>*Raman Spectroscopy in Carbons: From Nanotubes to Diamond*, edited by A. C. Ferrari and J. Robertson, special issue in *Philos. Trans. R. Soc. London, Ser. A* **362**, 2267 (2004).
- <sup>9</sup>F. Tuinstra and J. L. Koenig, *J. Chem. Phys.* **53**, 1126 (1970).
- <sup>10</sup>A. C. Ferrari and J. Robertson, *Phys. Rev. B* **61**, 14095 (2000); **64**, 075414 (2001).
- <sup>11</sup>C. Thomsen and S. Reich, *Phys. Rev. Lett.* **85**, 5214 (2000).
- <sup>12</sup>S. Pisana, M. Lazzeri, C. Casiraghi, K. Novoselov, A. K. Geim, A. C. Ferrari, and F. Mauri, *Nat. Mater.* **6**, 198 (2007).
- <sup>13</sup>A. Das, S. Pisana, S. Piscanec, B. Chakraborty, S. K. Saha, U. V. Waghmare, R. Yang, H. R. Krishnamurthy, A. K. Geim, A. C. Ferrari, and A. K. Sood, arXiv:cond-mat/0709.1174v1.
- <sup>14</sup>J. Yan, Y. B. Zhang, P. Kim, and A. Pinczuk, *Phys. Rev. Lett.* **98**, 166802 (2007).
- <sup>15</sup>M. Lazzeri and F. Mauri, *Phys. Rev. Lett.* **97**, 266407 (2006).
- <sup>16</sup>M. Lazzeri, S. Piscanec, F. Mauri, A. C. Ferrari, and J. Robertson, *Phys. Rev. B* **73**, 155426 (2006).
- <sup>17</sup>Y. Wu, J. Maultzsch, E. Knoesel, B. Chandra, M. Huang, M. Y. Sfeir, L. E. Brus, J. Hone, and T. F. Heinz, *Phys. Rev. Lett.* **99**, 027402 (2007).
- <sup>18</sup>K. T. Nguyen, A. Gaur, and M. Shim, *Phys. Rev. Lett.* **98**, 145504 (2007).
- <sup>19</sup>K. S. Novoselov, A. K. Geim, S. V. Morozov, D. Jiang, Y. Zhang, S. V. Dubonos, I. V. Grigorieva, and A. A. Firsov, *Science* **306**, 666 (2004).
- <sup>20</sup>Y. Y. Zhang, Y. W. Tan, H. L. Stormer, and P. Kim, *Nature (London)* **438**, 201 (2005).
- <sup>21</sup>A. Gupta, G. Chen, P. Joshi, S. Tadigadapa, and P. C. Eklund, *Nano Lett.* **6**, 2667 (2006).
- <sup>22</sup>D. Graf, F. Molitor, K. Ensslin, C. Stampfer, A. Jungen, C. Hierold, and L. Wirtz, *Nano Lett.* **7**, 238 (2007).
- <sup>23</sup>Y. W. Tan, Y. Zhang, K. Bolotin, Y. Zhao, S. Adam, E. H. Hwang, D. Das Sarma, H. L. Stormer, and P. Kim, arXiv:cond-mat/0707.1870.
- <sup>24</sup>J. Martin, N. Akerman, G. Ulbricht, T. Lohmann, J. H. Smet, K. von Klitzing, and A. Yacoby, arXiv:cond-mat/0705.2180.
- <sup>25</sup>S. Piscanec, M. Lazzeri, F. Mauri, A. C. Ferrari, and J. Robertson, *Phys. Rev. Lett.* **93**, 185503 (2004).
- <sup>26</sup>P. Lespade, A. Marchard, M. Couzi, and F. Cruege, *Carbon* **22**, 375 (1984).
- <sup>27</sup>A. C. Ferrari, *Solid State Commun.* **143**, 47 (2007).
- <sup>28</sup>L. Pietronero and S. Strassler, *Phys. Rev. Lett.* **47**, 593 (1981).
- <sup>29</sup>F. Schedin, A. K. Geim, S. V. Morozov, E. W. Hill, P. Blake, M. I. Katsnelson, and K. S. Novoselov, *Nat. Mater.* **6**, 652 (2007).